Journal of Water Process Engineering 76 (2025) 108137

Contents lists available at ScienceDirect

Journal of Water Process Engineering

journal homepage: www.elsevier.com/locate/jwpe

Leveraging naturally low pH for enhanced 2,4-dichlorophenoxyacetic acid removal from industrial wastewater: Carbon black adsorption and resource recovery approach

Noppaluck Promjan [a], Kullapa Soratana [b,*], Tanapon Phenrat [a,**]

[a] Research Unit for Integrated Natural Resources Remediation and Reclamation (IN3R), Department of Civil Engineering, Faculty of Engineering, Naresuan University, Phitsanulok 65000, Thailand
[b] Faculty of Logistics and Digital Supply Chain, Naresuan University, Phitsanulok 65000, Thailand

ARTICLE INFO

Editor: Xiaying Xin

Keywords:
Carbon black
2,4-dichlorophenoxyacetic acid
Adsorption
Global warming potential assessment
Cost analysis
Waste utilization

ABSTRACT

A sustainable approach for treating 2,4-dichlorophenoxyacetic acid (2,4-D) in acidic industrial wastewater was investigated by leveraging its naturally low pH characteristics. The adsorption performance of bare carbon black (CB) under acidic conditions was evaluated in comparison with 3-aminopropyltriethoxysilane (APTES)-modified CB, while exploring the integration of waste-derived sodium hydroxide (NaOH) for final pH adjustment. The results showed that optimal 2,4-D removal was achieved by bare CB at pH 2, aided by hydrogen bonding, electrostatic interactions, and Lewis acid–base interactions working synergistically. At pH 2, the maximum sorption capacity of 14 mg/g was observed at an optimal CB dose of 4.5 g/L. While APTES-modified CB at pH 4 had a 3.63-times higher sorption capacity, our life-cycle assessment revealed that utilizing bare CB under naturally acidic conditions coupled with waste-derived NaOH reduced the global warming potential by 27 % compared to using APTES-modified CB with fresh NaOH. This reduction primarily resulted from avoiding energy-intensive modification processes and utilizing waste-derived chemicals. The approach also decreased operational costs by 35 %. The adsorption process followed the Freundlich isotherm and pseudo-second-order kinetic models, indicating multi-layer adsorption and chemisorption mechanisms. This research demonstrates that integrating naturally occurring acidic conditions with waste-derived materials can enhance both environmental and economic sustainability in treating industrial wastewater under challenging pH conditions, supporting circular-economy principles in wastewater treatment.

1. Introduction

2,4-dichlorophenoxyacetic acid (2,4-D) is extensively utilized worldwide as a key ingredient in approximately 1500 agricultural and home-use herbicides, functioning as a mimic of natural plant auxins to regulate plant growth [1,2]. Its widespread application spans across developed and developing nations, with significant production volumes reported in various countries. For instance, China produced 40,000 tons of 2,4-D in 2010, while Brazil consumed 57,389.35 tons in 2017, ranked as their second most-used pesticide after glyphosate [3,4]. Notably, in Thailand, particularly in the flatlands of Nakhon Sawan province, 2,4-D usage is pronounced, particularly in the cultivation of sugarcane and cassava [5].

Despite its widespread application, numerous studies have underscored the adverse effects of 2,4-D on both animal and human health. It is classified as a moderately hazardous substances (in Group II of the World Health Organization classification), with a median lethal dose range of 138 to 150 mg/kg in rats [6]. Furthermore, 2,4-D is identified as a human carcinogen and an endocrine disruptor [5,6].

A critical environmental challenge has also emerged from 2,4-D production facilities, which generate highly acidic wastewater (pH ≈ 1.0) containing elevated concentrations of 2,4-D (40–6000 mg/L), and have a high chemical oxygen demand (20,000–40,000 mg/L) and chloride content (17,000–30,000 mg/L) [7]. Inadequate treatment of such contaminated effluents can lead to the contamination of surface water sources [1,5,8]. Due to its high water solubility (33,900 mg/L)

* Correspondence to: K. Soratana, Faculty of Logistics and Digital Supply Chain, Naresuan University, Phitsanulok 65000, Thailand.
** Correspondence to: T. Phenrat, Department of Civil Engineering, Faculty of Engineering, Naresuan University, Phitsanulok 65000, Thailand.
E-mail addresses: kullapas@nu.ac.th (K. Soratana), pomphenrat@gmail.com (T. Phenrat).

https://doi.org/10.1016/j.jwpe.2025.108137
Received 1 February 2025; Received in revised form 20 May 2025; Accepted 9 June 2025
Available online 25 June 2025

and low volatility (vapor pressure 1.4 × 1^{-7} mmHg), 2,4-D poses a significant threat for surface water contamination compared to other environmental media. Exhibiting notable environmental persistence, 2,4-D demonstrates a half-life ranging from 15 to 312 days in aqueous environments. In natural settings, beyond its inherent toxicity, 2,4-D undergoes degradation processes that transform it into other harmful substances. Aerobic organisms, such as *Azotobacter chroococcum* and fungi [1], play crucial roles in breaking down 2,4-D, sequentially converting it into 2,4-dichlorophenol (2,4-DCP), 4-chlorophenol, and 2,4-dichloro-cis,cis-muconate [1,6], all of which are also toxic. Anaerobic processes similarly contribute to 2,4-D degradation, transforming it into 2,4-DCP and carbon dioxide. However, the microbial degradation of 2,4-D is limited, emphasizing the need to prevent its release into the environment to mitigate adverse impacts on both animal and human health.

To address the need for environmental protection and to meet stringent groundwater and drinking water standards (the 30 μg/L threshold for 2,4-D in Thailand [5] and the 100 μg/L threshold for 2,4-D in Canada [9]), the demand for cost-effective and sustainable treatment methods for industrial wastewater contaminated with high concentrations of 2,4-D has increased. Moreover, the inherently low pH characteristic of 2,4-D wastewater necessitates the development of unique treatment approaches that can effectively operate under acidic conditions because conventional neutralization requires substantial quantities of chemicals and generates additional waste streams.

Recent studies have explored various advanced treatment approaches, including nanoscale MIL-53(Al) (removal efficiency 83 %), magnetic nanoparticles with amino functional groups (Fe_3O_4@SiO_2-NH_2), and carbon nanotubes (removal efficiency 97.96 %) [10–12]. However, these advanced materials require a pH adjustment to neutral or near-neutral conditions in addition to their complex synthesis procedures involving multiple chemical steps, potentially increasing both operational costs and environmental impacts.

Among carbon-based sorbents applicable in 2,4-D removal, carbon black (CB) is emerging as a promising sustainable solution, particularly when derived from waste tires through pyrolysis. Carbon black offers significantly lower carbon dioxide (CO_2) emissions (2.19 tons per ton of CB) compared to other adsorbents, such as granular activated carbon (20 tons), multi-walled carbon nanotubes (210 tons), and single-walled carbon nanotubes (480 tons) [13–15]. Previous research, focusing primarily on adsorption efficiency and innovation, has investigated CB modified with aminopropyltriethoxysilane (APTES) at pH 4, achieving a 2.5-times higher sorption capacity than bare CB [16]. However, no comparative analysis in terms of sustainability and cost-effectiveness of APTES-modified CB versus bare CB at low pH values has been performed.

Drawing insights from sustainable waste management practices, as demonstrated by Mooheng et al. [44], who achieved significant cost reductions and environmental benefits through waste-derived chemical utilization, the application of bare CB at low pH for 2,4-D removal with waste-derived sodium hydroxide (NaOH) for final pH adjustment was inspired by their study while also being revised for use in this research. Mooheng et al. [44] showed that utilizing hydrochloric acid (HCl) waste in regenerating oil-contaminated sludge from metalworking fluid wastewater treatment via dissolved-air flotation reduced sludge disposal and coagulant costs by 15 % and diminished the global warming potential (GWP) by 80 % compared to conventional methods. This research suggests the potential that employing bare CB under acidic conditions, followed by neutralization with waste-derived NaOH, could offer similar environmental and economic advantages.

Therefore, this study examined: (1) the comparative techno-economic performance of bare CB under acidic conditions versus APTES-modified CB at the optimal pH; (2) the mechanisms and efficiency of 2,4-D adsorption onto CB under acidic conditions; and (3) the environmental and economic implications of using waste-derived alkaline materials for final pH adjustment. This research addresses the growing need for sustainable treatment methods that align with circular-economy principles while effectively managing industrial wastewaters with challenging pH conditions.

2. Materials and methods

To enable a comprehensive sustainability assessment comparing bare CB with waste-derived alkaline materials versus APTES-modified CB for 2,4-D removal, new experimental investigations and existing data from the literature were combined. While APTES-modified CB has been thoroughly characterized and its 2,4-D removal efficiency well documented at pH 4 [16], understanding the performance of bare CB under acidic conditions is still limited. Hence, the experimental studies on 2,4-D sorption with bare CB were thoroughly conducted by examining its physical and chemical characteristics, pH-dependent behavior, and operating parameters.

For the comparative assessment with APTES-modified CB, we utilized the established synthesis protocol and removal efficiency data from Legocka et al. [16], who reported comprehensively on material preparation, operating conditions, and treatment performance. The information to conduct comparative analyses of operational costs and environmental impacts, particularly the GWP, for both treatment approaches was sufficiently obtained from the existing dataset combined with the new experimental results for bare CB in this research. The following sections detail our experimental methods for bare CB characterization and 2,4-D removal, followed by the methodology for the sustainability assessment of both treatment options.

2.1. Chemicals and materials

All chemicals and materials utilized in this study were the commercial grade. Carbon black powder (Carbon black N660) was sourced from Thai Carbon Black Public Company (Angthong province, Thailand). The 2,4-D compound, with a purity of 95 %, was acquired from Pchemitech Company (Bangkok, Thailand). Deionized water with a resistivity of 18 MΩ cm was consistently used in all experiments.

The microstructure of the CB was characterized using a scanning electron microscope (SEM) (model LEO 1455 VP, UK) and the Brunauer–Emmett–Teller (BET) method (TriStar II 3020, USA) to investigate its particle morphology, specific surface area, and total pore volume. Additionally, Fourier transform infrared spectroscopy (FTIR) (PerkinElmer, Germany) was utilized to analyze the functional groups of the CB. Finally, the point zero charge (pH_{pzc}) of the CB was determined using a zeta potential analyzer (Malvern Zetasizer Nano-ZS ZEN 3600, UK) that measured the zeta potential of the dispersion over a pH range of 1–12. Additionally, the Zetasizer was utilized to analyze the particle size distribution of the CB dispersion.

2.2. Batch sorption experiment for bare CB

To investigate the influence of pH on 2,4-D sorption by bare CB, batch experiments were conducted at initial pH values of 2, 4, 6, 8, and 10. Dispersions were prepared in 200 mL Erlenmeyer flasks with a 2,4-D concentration of 20 mg/L and a CB dosage of 4.5 g/L. The flasks were then stirred at 120 rpm using a magnetic stirrer. Prior to analyzing the efficacy of the 2,4-D removal, the CB was separated from the dispersion using Whatman filter paper #42. Subsequently, the residual concentration of 2,4-D was measured using an ultraviolet–visible (UV–Vis) spectrometer (Genesys 10S UV–Vis spectrophotometer, Thermo Scientific, USA) at a wavelength of 230 nm [17].

To determine the optimal bare CB concentration for maximum 2,4-D sorption at pH 2 (the optimized pH), batch sorption experiments were conducted by varying the CB concentrations from 1.5 to 7.5 g/L while maintaining a 2,4-D concentration of 20 mg/L. These experiments were performed in flasks stirred at 120 rpm using a magnetic stirrer, with the residual 2,4-D concentrations measured by UV–Vis spectrometer every six hours. The sorbed concentration was then analyzed to ascertain the

optimal CB content. Subsequently, the determined optimal CB dose was utilized to construct an adsorption isotherm by varying the concentration of 2,4-D from 10 to 50 mg/L at pH 2, employing the same experimental setup and 2,4-D quantification approaches as in the preceding experiments.

2.3. Model of adsorption kinetics and adsorption isotherm

The amount of 2,4-D retained in the adsorbent phase was calculated as follows [18–20]:

$$q_t = V(C_o - C_t)/W \quad (1)$$

$$q_e = V(C_o - C_e)/W \quad (2)$$

where q_t and q_e (mg/g) are the amounts of 2,4-D adsorbed onto the carbon materials at time, *t,* and at equilibrium time, *e*, respectively; *V* is the suspension volume (in liters); C_0, C_t, and C_e (in milligrams per liter) are the aqueous 2,4-D concentrations at the initial time, *t,* and at equilibrium, *e*; and *W* (in grams) is the bare CB mass in the reactor being evaluated.

To evaluate the adsorption capacities of the 2,4-D on the CB, Langmuir and Freundlich isotherms were used to model the experimental data. The Langmuir adsorption isotherm indicates monolayer sorption onto a homogenous surface, as follows [20]:

$$q_e = Q_0 K_L C_e / 1 + K_L C_e \quad (3)$$

where Q_0 (in milligrams per gram) is the maximum monolayer coverage capacity; and K_L (in liters per milligram) is the Langmuir isotherm constant, and

$$R_L = 1/1 + K_L C_o \quad (4)$$

(where R_L is the separation factor), is calculated from the Langmuir isotherm. This value showed the favorable adsorption between the adsorbent and adsorbate, with $R_L > 1$ being unfavorable, $R_L = 1$ being linear, $0 < R_L < 1$ being favorable, and $R_L = 0$ being irreversible [21].

Contrastingly, the Freundlich adsorption isotherm assumes heterogeneous adsorption on the surface, as follows [20]:

$$q_e = K_f C_e^{\frac{1}{n}} \quad (5)$$

where K_f (in milligrams per gram) (milligrams per liter)$^{-n}$ is the Freundlich isotherm constant and is related to the adsorption capacity; and *n* is the intensity of the adsorption.

In addition, the 2,4-D adsorption kinetics on the CB were comparatively modeled using pseudo-first-order (Eq. (6)) and pseudo-second-order (Eq. (7)) models

$$\ln(q_e - q_t) = \ln q_e - k_1 t \quad (6)$$

$$\frac{t}{q_t} = \frac{1}{k_2 q_e^2} + \frac{1}{q_e} t \quad (7)$$

where k_1 is the sorption rate constant of the pseudo-first-order model; and k_2 is the sorption rate constant of the pseudo-second-order model [20].

2.4. Estimation of potential operational cost savings and GWP reduction

A comparative life-cycle assessment (LCA) was conducted to evaluate the potential greenhouse gas emissions and operational cost savings associated with three different scenarios for 2,4-D absorption. These experiments focused on contaminated water with a natural pH of 1, which is commonly observed in wastewater contaminated with 2,4-D. The three scenarios differed in the CB adsorption method and the source of chemicals used for pH adjustment, with an emphasis on reducing chemical consumption and utilizing waste-derived substances.

A gate-to-gate LCA was performed to quantify the GWP and the operational costs associated with the three scenarios. The functional unit of the LCA was defined as the adsorption of 42 mg of 2,4-D by CB (see the Supplementary information (SI) for a functional unit calculation), and the system boundaries for each scenario were limited to the processes involved in 2,4-D absorption and pH adjustment, excluding raw material acquisition and waste management, as illustrated in Fig. 1.

The contaminated water used in all three scenarios had a naturally low pH of 1. Scenario 1 utilized CB modified with APTES in the absorption process, based on an experiment conducted by Legocka et al. [16], to evaluate the 2,4-D absorption capability of CB. The pH of the water was adjusted from 1 to 4 using 100 mL (or 113 g) of fresh NaOH (1 M, 99 % by weight). The modified CB, derived from 0.2 g of APTES and 2 g of CB, was shaken for two hours and added to the pH 4-contaminated water, followed by stirring for 3 h to allow for solvent evaporation. The treated water was then subjected to a pH adjustment by mixing it with 0.1 mL (or 0.113 g) of NaOH (1 M, 99 % by weight) to achieve a pH of 7.

Scenarios 2 and 3 diverged from Scenario 1 in their use of 4.5 g/L of CB for 2,4-D adsorption at a pH of 2. However, Scenarios 2 and 3 (Fig. 1b) shared similarities, the primary distinction being in the source of the alkali used for pH adjustment. Scenario 2 employed fresh NaOH (99 % by weight) to adjust the pH from 1 to 2, and to neutralize the treated water to a pH of 7, whereas Scenario 3 involved the use of NaOH from waste streams, such as spent pot liner from aluminum electrolysis (NaOH 25 % by weight) [22] (Fig. 1b), but otherwise followed the same steps as Scenario 2.

In Scenario 2, the pH of the contaminated water was adjusted from 1 to 2 using 90 mL (102 g) of fresh NaOH (1 M, 99 % by weight). Subsequently, 4.5 g/L of CB was added and the mixture was stirred for 6 h. Afterward, the pH of the treated water was neutralized to 7 by adding 10 mL (11.3 g) of fresh NaOH (1 M, 99 % by weight). In Scenario 3, to adjust the pH of the contaminated water from 1 to 2, 92 mL (104 g) of NaOH from waste streams was used. After the adsorption process, the pH of the treated water was neutralized to pH 7 using 10 mL (11.3 g) of NaOH waste (1 M, 25 % by weight).

A life-cycle inventory (LCI) analysis involves compiling data and information from various sources to assess the environmental impacts of a product or process throughout its life cycle. In this step, the inventory was gathered primarily from experiments conducted by Legocka et al. [16] and through calculations. The specific data and information needed for the LCI analysis are detailed in Table S4 in the SI.

In the life-cycle impact assessment (LCIA), the GWP across the three distinct life-cycle scenarios of 2,4-D absorption processes was evaluated. The GWP was computed by multiplying activity data and emissions factors. The activity data we used were derived from calculations based on available data in the LCI step, while the emissions factors for each product and process were sourced from databases, such as ecoinvent v.2.2, the Intergovernmental Panel on Climate Change 2007, and the Thai National Database. The LCIA method employed was the ReCiPe 2016 Midpoint (E) V1.08/ World (2010) E model, accessible in SimaPro v.9.0.5.2 software. The emissions factors used are listed in Table S5.

To conduct the operational cost analysis, the average market prices of CB, APTES, HCl, NaOH, and electricity were obtained from a Thai market survey. The mass balance of chemicals consumed and waste generated in each step of each treatment scenario were calculated based on the information provided in the LCI table (Table S4). These mass balance values were then multiplied by the average market prices to determine the total operational cost for each scenario. The information needed for the potential operational cost savings analysis is detailed in Table S3.

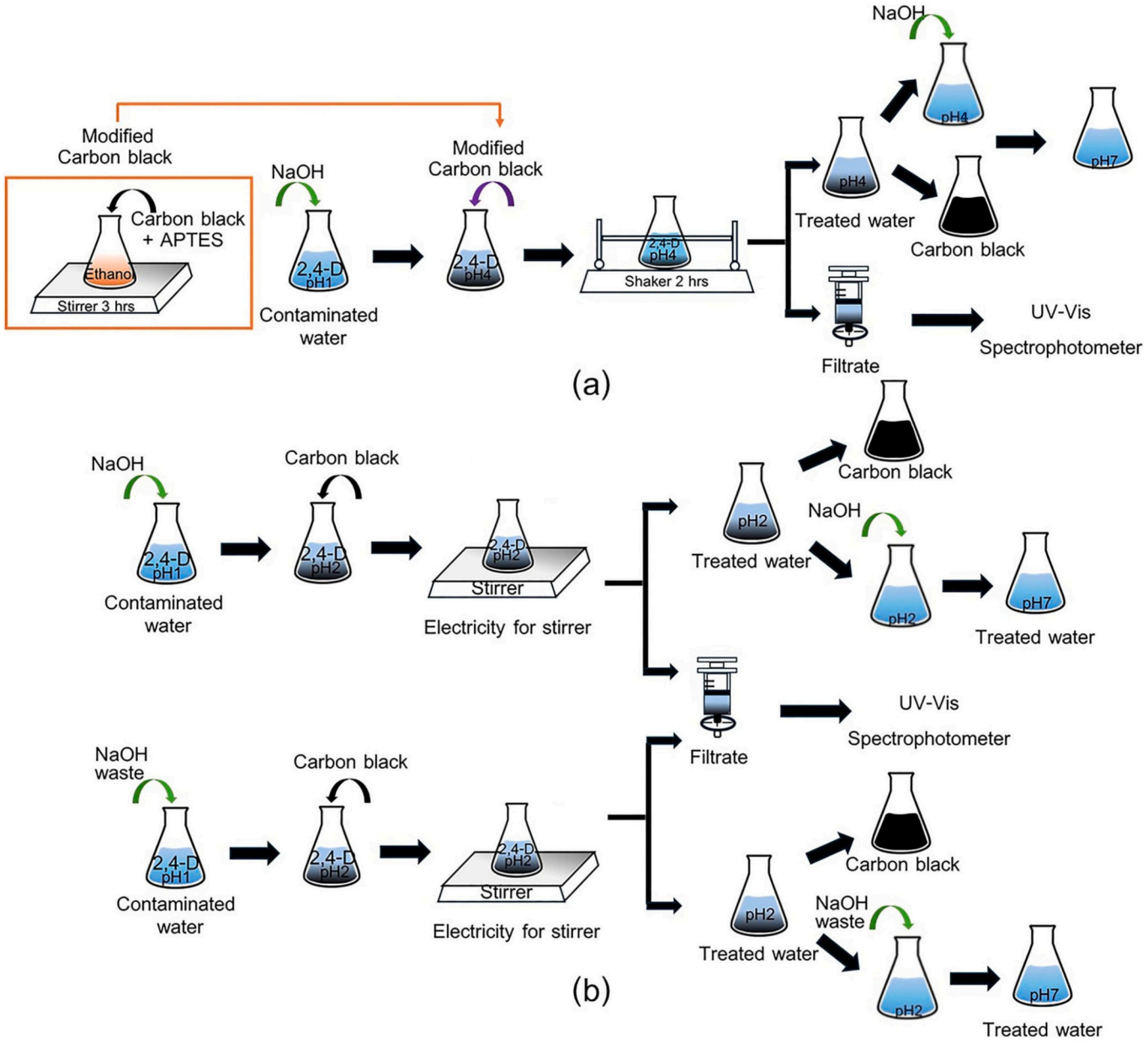

Fig. 1. Summary of the three evaluated scenarios: (a) APTES-modified CB; and (b) fresh or waste HCl and NaOH.

3. Results and discussion

3.1. Physical and chemical characteristics of CB

As depicted in Fig. 2a, the SEM micrograph displays individual CB particles with an average diameter of 200 nm. However, the micrograph also shows the agglomeration of CB into clusters ranging from 200 to 1400 nm in diameter. This observation aligns well with the intensity-averaged diameter of CB in a dispersion at pH 2, as measured by dynamic light scattering (Fig. 2b), ranging from 110 to 1100 nm with an average diameter of 500 nm.

As shown in Fig. 2a, the CB surface appears rough, although it lacks discernible pores, which aligns well with the low total pore volume of 0.03 cm^3/g and the absence of micropores, as measured by BET (Table S1). The surface area of the CB was determined to be 33.39 m^2/g. These physical characteristics corroborate its nonporous nature, as previously reported in the literature [23].

Fig. 2c depicts the relationship between the pH of CB dispersion and its corresponding zeta potential across the pH range from 2 to 12. At a pH of 12, the maximum negative zeta potential of CB was −41.80 mV, whereas at a pH of 2, the maximum positive zeta potential was 43.30 mV. The point of zero charge of CB was determined to be at a pH of 6.5, which closely aligns with the findings of [24,25]. Consequently, below a pH of 6.5, the surface of CB possesses a positive charge.

Fig. 3 shows the FTIR analysis of the bare CB, revealing the presence of six primary interfacial functional groups—alcohol, phenol, carboxylic (C—O and O═H), ketone (C=O), aromatic hydrocarbons (C=C), and carbonyl (C=O). These functional groups were corroborated by the corresponding wavenumbers of their vibrations, as detailed in Table S2. The occurrence of these functional groups in bare CB aligns with the results of [26]. Interestingly, the O═H functional group at 3796 cm^{-1} may represent the stretching of the silanol (SiOH) group [27], suggesting the CB has been contaminated with silica (SiO_2) from recycled tire waste [28].

The negative zeta potential of CB, shown in Fig. 2c, can presumably be attributed to the deprotonation of carboxyl and hydroxyl functional

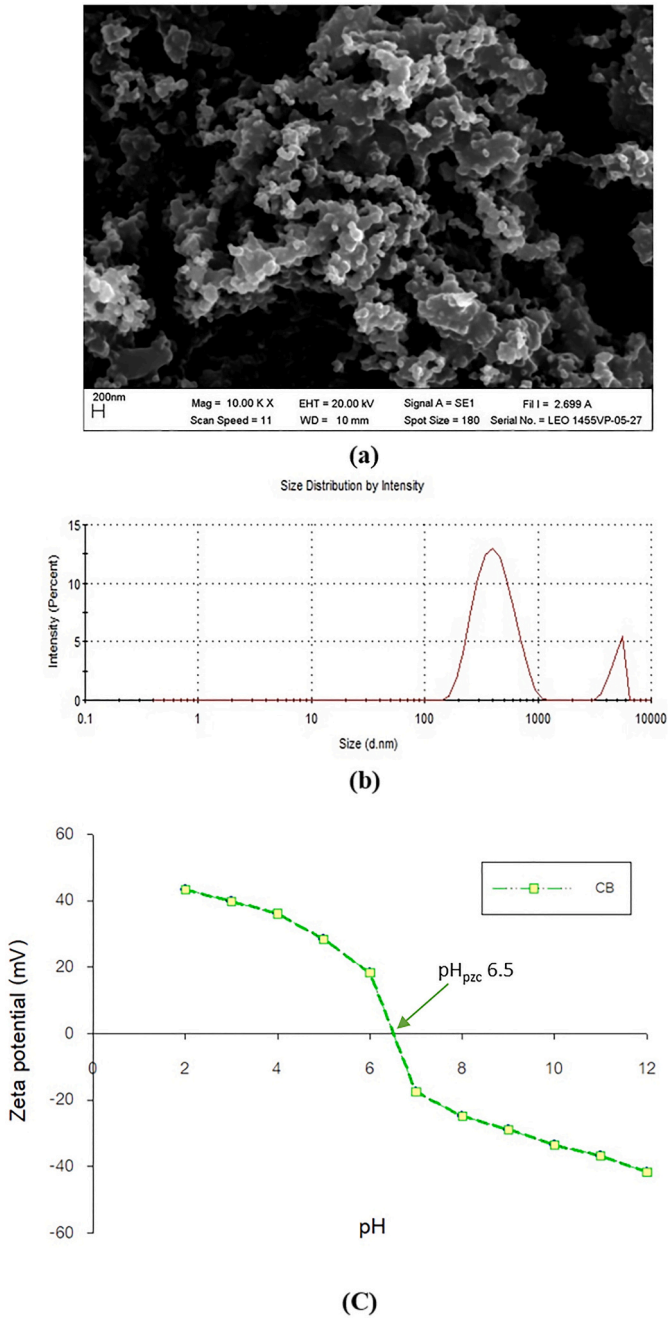

Fig. 2. (a) SEM micrograph of CB surface; (b) particle size distribution of CB dispersion at pH 2 measured by dynamic light scattering; and (c) relationship between zeta potential and pH of CB dispersion.

groups, with the positive zeta potential likely being a result of the protonation of these same functional groups [29]. These functional groups are also implicated in facilitating the sorption of 2,4-D through hydrogen bonding [30] and π–π electron donor–acceptor interactions [31], which we expound upon later in the discussion.

3.2. *Effect of solution pH on 2,4-D adsorption*

The physicochemical mechanisms underlying the role of acidic pH in the sorption of 2,4-D by CB, building on Legocka et al.'s [16] [16] previous observation of this phenomenon was elucidated in this section. First, as shown in Fig. 4 at all pH levels, the initial rapid adsorption phase (0−1h) can be attributed to the abundance of available active sites on the CB surface and the strong concentration gradient driving mass transfer. Microscopic analysis of this process suggests a boundary layer diffusion mechanism initially controlling the rate, followed by intra-particle diffusion as adsorption progresses. The observed plateau after 4–6 h indicates the establishment of a dynamic equilibrium where the rates of adsorption and desorption become equal. Therefore, the optimal adsorption time for this process is 6 h. The adsorption kinetics model will be further discussed in the modeling section.

Furthermore, Fig. 4 shows that the sorption capacity (q) of 2,4-D onto CB in the steady state increases with decreasing pH in the CB dispersion. Specifically, the q values rise from 5 mg/g at pH 10 to 14 mg/g at pH 2 (Fig. S1). Mechanistically, the sorption of 2,4-D on a sorbent is driven by hydrogen bonding interactions, electrostatic interactions, π–π electron donor–acceptor interactions [30,31], and Lewis acid–base interactions [32], with the first three interactions being influenced by the pH of the dispersion. Therefore, analyzing the roles of pH in these interactions can light on the experimental findings.

Fig. 5 depicts the potential interactions between 2,4-D and the functional groups of CB, both influenced by pH. At pH 2, the majority (90 %) of 2,4-D exists in a molecular (uncharged) form, while 10 % is in an anionic form. Conversely, CB exhibited the highest proportion of positively charged sites (as confirmed by the highest zeta potential of 43.30 mV), theoretically explained by functional groups, including carboxyl and hydroxyl, becoming protonated [29]. Consequently, at this pH, hydrogen bonding interactions between -OH on the CB and 2,4-D presumably occur at maximum intensity. Similarly, electrostatic interaction occurred between the positively charged carboxyl and hydroxyl functional groups ($-OH_2^+$) on the CB and negatively charged oxygen and hydroxyl groups ($=O^-$) on the 2,4-D. Additionally, Lewis acid–base interaction took place between the halogen group of the 2,4-D (as a Lewis base) and the carboxyl group of the CB (as a Lewis acid). The combined potential of these three interactions explains the maximum 2,4-D sorption capacity of 14 mg/g (Figs. 5b and S2).

At the molecular level, these interactions can also be visualized and supported as follows: protonated carboxyl groups ($–COOH_2^+$) on the CB surface form strong electrostatic bonds with the partially deprotonated carboxyl groups of 2,4-D molecules. Simultaneously, the chlorine atoms in 2,4-D, due to their high electronegativity, create localized areas of negative charge that interact with the positively charged regions of the CB surface. Density Functional Theory (DFT) calculations reported by Wu et al.'s [32] for similar systems suggest binding energies of approximately −42 to −65 kJ/mol for these electrostatic interactions at pH 2, compared to only −15 to −25 kJ/mol at pH 10. Additionally, the aromatic ring in 2,4-D can participate in π-stacking interactions with graphitic domains on the CB surface, particularly in regions where surface oxygen groups have modified the electron density of the carbon structure. These π-stacking interactions contribute approximately 20–30 % of the total binding energy at pH 2 based on comparable carbon-based adsorbent studies [31].

Fig. 3 shows the FTIR analysis, which illustrates the change in functional groups on the CB after 2,4-D sorption, supporting the proposed interactions at pH 2. For instance, after 2,4-D sorption, there was a decline in OH groups on the CB, as can be seen from the increase in transmittance at a wavenumber of 3736 cm^{-1}, potentially representing the stretching mode of SiOH [27], and in a wavenumber range of 3000–3600 cm^{-1}, representing stretching of the alcohol, phenol, carboxylic acid, and hydroxyl groups on the CB. The decrease in stretching mode of these OH groups support their coordinated interactions with 2,4-D via the three mechanisms described above. In addition, the peak at 2325 to 2311 cm^{-1} representing the C═O group and the decrease in transmittance from 2500 to 3000 cm^{-1} following 2,4-D sorption onto the CB indicates an increase in C═O [33] and O═H [34] stretching, potentially from the carbonyl and hydroxyl groups of the sorbed 2,4-D, respectively. Notably, the peak at 2500 to 3000 cm^{-1} appears in the spectrum of the 2,4-D [35]. Thus, the appearance of this peak on the 2,4-D-sorbed CB confirms the sorption of 2,4-D.

Beyond the observations already discussed, further analysis of the

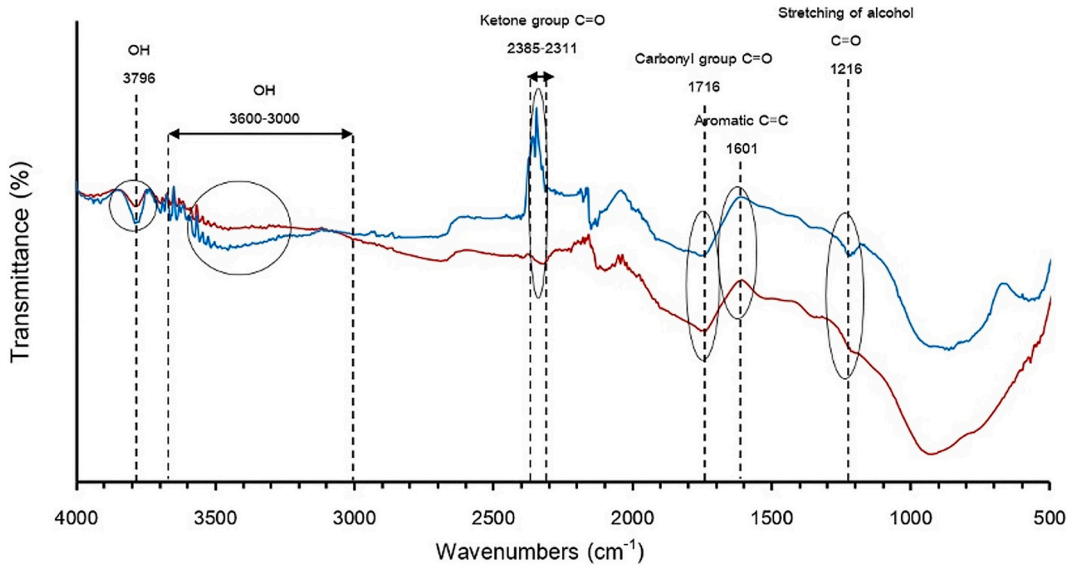

Fig. 3. FTIR analysis of CB and CB after 2,4-D sorption.

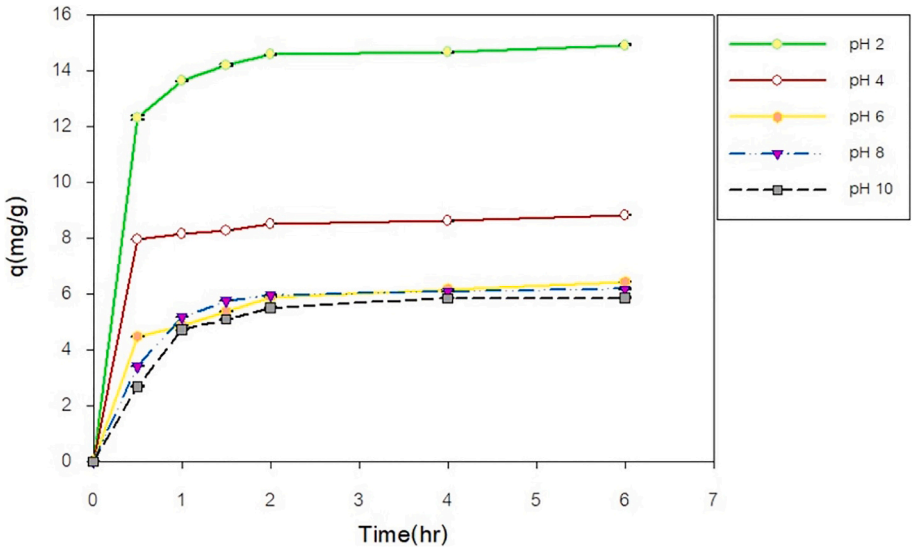

Fig. 4. Effect of pH on the efficiency of 2,4-D removal by CB. Initial dissolved 2,4-D concentration = 20 mg/L and CB concentration = 4.5 g/L at 25 °C.

FTIR spectra provides additional mechanistic insights. The changes observed around 1601 cm^{-1}, corresponding to aromatic C—C vibrations, suggest the involvement of the aromatic ring of 2,4-D in the adsorption process, likely through π-π interactions with graphitic domains on the CB surface. The relative intensity changes in the carbonyl region (around 1716 cm^{-1}) before and after adsorption provide spectroscopic evidence for the participation of these groups in hydrogen bonding interactions. These spectral observations, when considered together, confirm that multiple functional groups on both the adsorbent and adsorbate participate simultaneously in the adsorption process, creating a complex but highly effective binding interface particularly under acidic conditions. However, at pH 4, although a larger fraction of the 2,4-D becomes anionic, the CB exhibits reduced positive surface charge. Surprisingly, the 2,4-D sorption capacity decreased to 11.2 mg/g, even though the Lewis acid–base and hydrogen bonding interactions at this pH should not substantially differ from those at pH 2. Consequently, this reduction in 2,4-D sorption onto CB at pH 4 was attributed to the decrease in positively charged sites on the CB, thereby diminishing its electrostatic interactions with the 2,4-D. More importantly, at pH 10, where all the 2,4-D becomes anionic, the CB also becomes negatively charged, leading to electrostatic repulsion that counteracts the hydrogen bonding and Lewis acid–base interactions. This would account for the lowest 2,4-D sorption capacity among the four pH values studied. Comparative analysis of the observed 2,4-D sorption and the potential contribution of the three forces at three different pH levels offered a clear explanation of the poorer 2,4-D removal at neutral and alkaline pH values.

3.3. *Effect of CB dosages and initial 2,4-D concentrations*

Fig. 6a depicts the 2,4-D sorption capacity (q) as a function of CB dosage ranging from 1.5 to 7.5 g/L at an initial 2,4-D concentration of 20 mg/L and at the optimal pH of 2. The q values increased from 12.89 to 15.52 mg/g as the CB dose increased from 1.5 to 4.5 g/L. However, further increases in the CB dosage, from 4.5 to 7 g/L, resulted in a decrease in the q value to 14.65 mg/g. Thus, at this initial 2,4-D concentration, the optimal CB dose was determined to be 4.5 g/L.

In contrast, Fig. 6b illustrates the 2,4-D sorption capacity (q) in

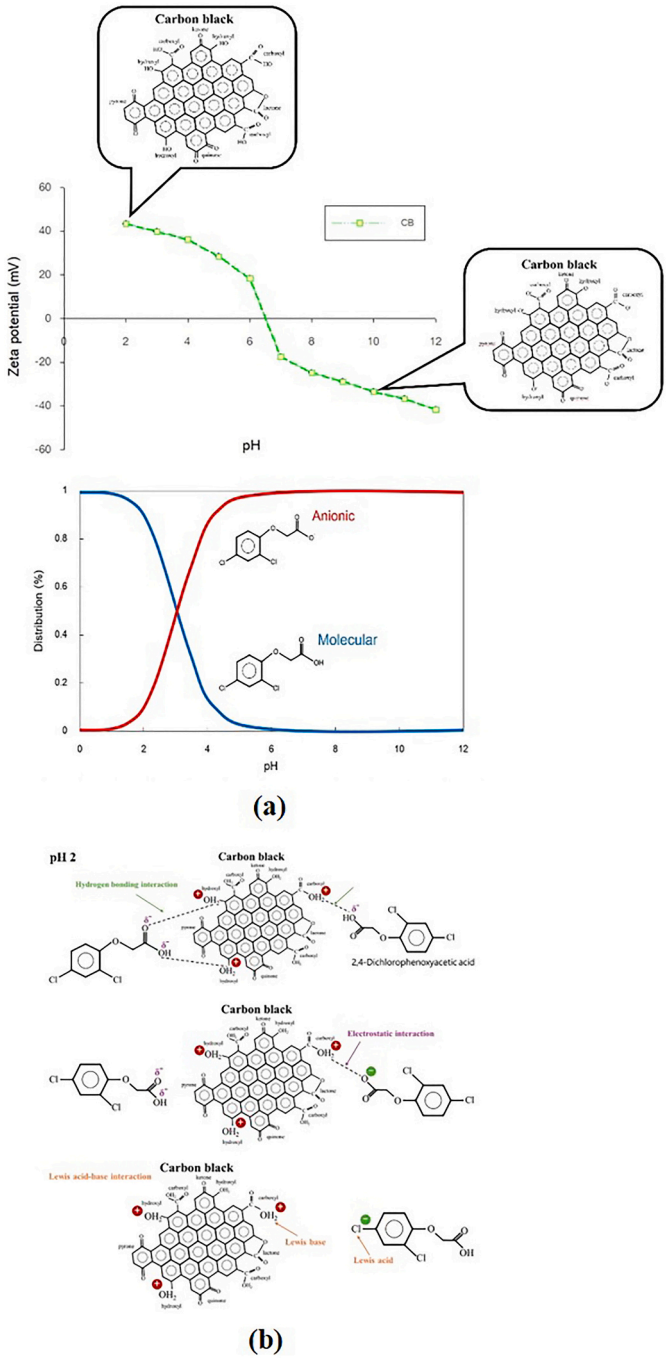

Fig. 5. (a) Protonation and deprotonation of the CB in terms of zeta potential and distribution; and (b) mechanism of the CB at pH 2.

relation to the initial 2,4-D concentrations, ranging from 10 to 50 mg/L, with the optimal bare CB dose set at 4.5 g/L and the optimal pH at 2. Evidently, that higher initial 2,4-D concentrations correspond to higher q values at equilibrium. The q values escalated from 1.18 to 9.35 mg/g as the 2,4-D concentrations increased from 10 to 50 mg/L. Notably, upon comparing the maximum q value achieved by the bare CB at pH 2 (9.35 mg/g) with that of CB modified with APTES at pH 7 (34 mg/g) from Legocka et al. [16] for a comparable 2,4-D concentration (50 mg/L), this study found that the CB modification with APTES outperformed the acid pH by approximately 3.63 times.

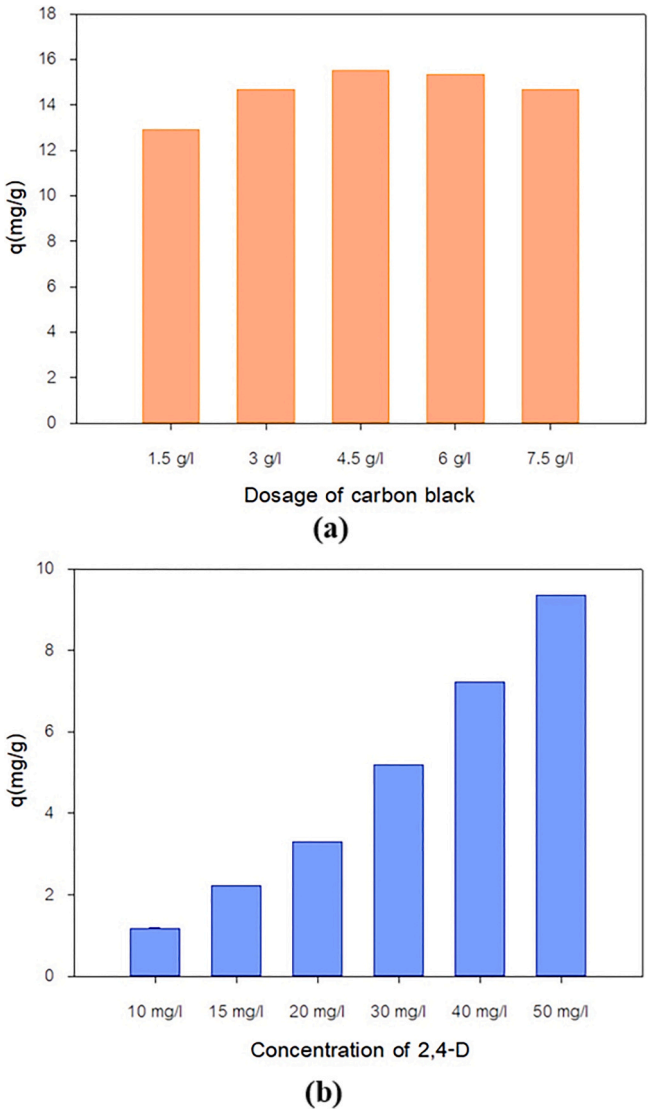

Fig. 6. (a) Effect of dosage sorption of 2,4-D on CB; and (b) adsorption capacity on CB of initial 2,4-D concentration.

3.4. Modeling the adsorption isotherm

Table 1 presents a summary of the equilibrium modeling outcomes for all the sorption experiments (see also Fig. S4) using the Langmuir and the Freundlich models. Remarkably, the r^2 value obtained from the Freundlich isotherm (0.942) substantially exceeded that from the Langmuir isotherm (0.790), indicating that the multi-layer and heterogeneous adsorption concept of the Freundlich isotherm better represents our experimental results. This observation aligns with the multi-point, non-homogeneous nature of CB, as confirmed by FTIR.

Thermodynamic analysis based on the Freundlich isotherm provides deeper insights into the adsorption mechanisms observed in the FTIR analysis. Using the Freundlich parameters from Table 1 (KF and $1/n$ = 3.54), the Gibbs free energy change (ΔG°) for the adsorption process at pH 2 was determined to be approximately −20.8 kJ/mol, indicating a

Table 1
The isotherms of the adsorption.

Materials	Langmuir isotherm			Freundlich isotherm		
	q_m(mg/g)	K_L	R^2	K_F	1/n	R^2
CB	1.06	0.11	0.790	263.03	3.54	0.942

spontaneous process. This value falls within the range typically associated with physical adsorption (−20 to −40 kJ/mol) and corresponds with the multi-mechanism model proposed from the FTIR analysis.

As discussed earlier, the FTIR spectroscopic evidence showing changes in the OH groups (3000–3600 cm^{-1}), carbonyl region (around 1716 cm^{-1}), and aromatic C—C vibrations (around 1601 cm^{-1}) collectively supports the multi-site, heterogeneous adsorption mechanism indicated by the better fit of the Freundlich model ($r^2 = 0.942$). The unfavorable adsorption suggested by the 1/n value of 3.54 aligns with our FTIR observations of competing interactions between the polar 2,4-D molecules and water for the various functional groups on the CB surface [36]. This competition is evidenced by the complex changes in the FTIR spectra, particularly in the hydroxyl region.

Furthermore, the superior fit of the Freundlich model compared to the Langmuir model ($r^2 = 0.790$) is consistent with the multiple interaction mechanisms identified through FTIR analysis—namely, hydrogen bonding, electrostatic interactions, and Lewis acid-base interactions—occurring simultaneously at different sites on the heterogeneous CB surface. The presence of diverse functional groups on CB (alcohol, phenol, carboxylic, ketone, aromatic, and carbonyl) as confirmed by FTIR (Fig. 3) provides multiple potential adsorption sites with varying energies, which explains the heterogeneous adsorption behavior better described by the Freundlich model. This contrasts with the APTES-modified CB at pH 7 reported by Legocka et al. [16], where the more favorable adsorption ($1/n = 0.574$) was primarily driven by a single dominant mechanism—the electrostatic attraction between the positively charged APTES groups and the anionic 2,4-D [16].

3.5. Modeling the sorption kinetics

The pseudo-first- and pseudo-second-order models were employed to simulate the kinetics of 2,4-D sorption. Table 2 provides a summary of the kinetic parameters derived from the modeling, encompassing the sorption capacity (qe modeled), rate constants (k_1 and k_2 for the pseudo-first- and pseudo-second-order models, respectively), and the r^2 values. As depicted in Fig. S3, the pseudo-second-order model exhibited superior fitting to the experimental data, as indicated by its high r^2 values, ranging from 0.99 to 1, suggesting its appropriateness for modeling 2,4-D sorption kinetics by CB at pH 2. The underlying premise of the pseudo-second-order kinetic model posits that the governing step is chemical sorption or chemisorption—a notion that aligns well with the observed behavior of 2,4-D sorption onto the CB, as has been discussed previously [37]. Notably, the sorption capacity at equilibrium predicted by the pseudo-second-order model closely matched the experimental values, ranging from 1.05 to 9.16 mg/g across the initial 2,4-D concentrations, spanning from 10 to 50 mg/L. The rate constant, k_2, exhibited a decrease with escalating initial concentration (e.g., the k_2 decreased from 9.33 at an initial concentration of 10 mg/L of 2,4-D to 0.88 at 50 mg/L of 2,4-D). This trend suggests that the sorption of 2,4-D occurred more rapidly at lower initial concentrations, consistent with findings from a previous study on the sorption of 2,4-D onto termite mound soil [38]. Interestingly, a comparison with the rate constant for 2,4-D sorption by CB modified with APTES at pH 7, and at an initial concentration of 110 mg/L, by Legocka et al. [16] revealed that the rate constant for bare CB at pH 2 under the same conditions was 1.73 times faster.

Table 2
Kinetic parameters of the pseudo-first-order, pseudo-second-order adsorption rate constants, and calculating and experimental of qe values obtained from different initial 2,4-D concentrations.

Initial con. (mg/L)	q_e exp. (mg/g)	Pseudo-first-order kinetic model			Pseudo-second-order kinetic model		
		k_1 (h^{-1})	q_e, calc. (mg/g)	R^2	k_2 (g mg^{-1} h^{-1})	q_e, calc. (mg/g)	R^2
10	1.04	0.494	0.13	0.893	9.33	1.05	0.999
15	2.07	0.853	0.17	0.828	9.75	2.09	1.000
20	3.02	1.384	0.48	0.996	7.06	3.05	1.000
30	5.06	0.562	0.28	0.938	5.32	5.08	1.000
40	7.00	0.568	0.81	0.965	1.75	7.06	1.000
50	9.04	0.488	1.41	0.965	0.88	9.16	1.000

3.6. Avoidance effects of the GWP

An attributional LCA was conducted for the three 2,4-D absorption scenarios. Scenario 1, involving CB modified with APTES and using fresh NaOH, had the highest GWP contribution among the three scenarios, with 0.6518 kg CO_2-eq per functional unit (42 mg of 2,4-D absorbed). Scenario 2, utilizing CB with fresh NaOH, yielded a GWP contribution of 0.1800 kg CO_2-eq per functional unit and Scenario 3, employing CB with NaOH from waste streams, had the lowest GWP contribution at −0.0748 kg CO_2-eq per functional unit. Scenarios 2 and 3 accounted for 13 % and 9 % of the total GWP from Scenario 1, respectively. The LCIA results for the three scenarios of 2,4-D absorption are illustrated in Fig. 7.

The primary GWP contribution from Scenario 1 stemmed from electricity consumption, which constituted approximately 80 % of its total GWP. Two energy consumption processes played significant roles in this—the stirrer in the mixing of the wastewater and modified CB and the shaker in preparing the modified CB, accounting for 3 % and 77 % of Scenario 1's total GWP, respectively. The secondary GWP contribution from Scenario 1 was from the fresh NaOH, accounting for 21 % of its total GWP. The fresh NaOH was used in two processes—sample preparation and the sample after adding CB, resulting in 19 % and 0.02 % of Scenario 1's total GWP, respectively.

Conversely, for Scenario 2, the primary GWP contribution originated from the fresh NaOH, accounting for 70 % of its total GWP, used for pH adjustment in the sample preparation process and the process after adding the CB, and contributing 63 % and 7 % of Scenario's 2 total GWP, respectively. The second highest GWP contribution originated from electricity consumption—the stirrer in the mixing of wastewater and CB—accounting for 25 % of Scenario 2's total GWP.

Similarly to Scenario 1, the major GWP contribution from Scenario 3 was from electricity consumption from the stirrer in the mixing of the wastewater and CB, accounting for 60 % of its total GWP. Notably, Scenario 3 had the lowest GWP among the three scenarios, with a total avoided GWP of 0.0745 kg CO_2-eq per functional unit. This is due to an avoided GWP of 71 % of its total GWP from the utilization of NaOH from waste streams. In Scenario 3, 7.06 M of NaOH waste was employed in

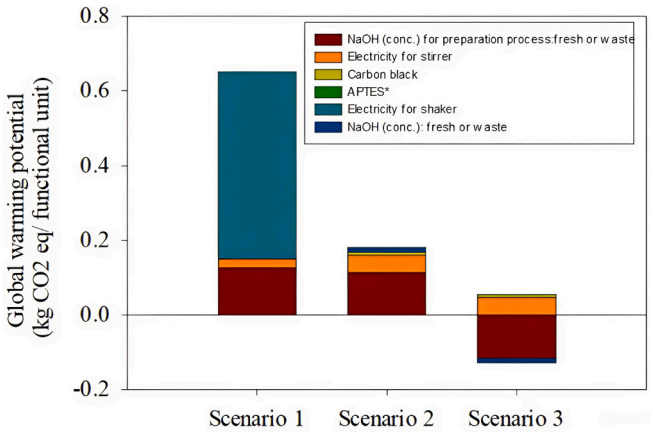

Fig. 7. Global warming potential of the three 2,4-D absorption scenarios investigated in this study.
Scenario 1: Modified carbon black with fresh NaOH.
Scenario 2: Carbon black with fresh NaOH.
Scenario 3: Carbon black with alkaline from waste streams.

the pH adjustment process, thus avoiding the need for 115.3 g of fresh NaOH (contributing 0.1285 kg CO_2-eq per functional unit). The GWP of fresh NaOH was avoided in the sample preparation process, contributing 0.1159 kg CO_2-eq per functional unit, and in the process after adding the CB, contributing 0.0126 kg CO_2-eq per functional unit.

A comprehensive examination of Scenario 3, incorporating the consequential LCA, revealed significant opportunities for mitigating GWP through strategic adjustments in chemical utilization. Specifically, by substituting fresh NaOH with repurposed NaOH (pH 13) sourced from waste streams, additional GWP reduction can be achieved. The GWP reduction observed in the consequential LCA of Scenario 3 amounted to 0.1141 kg CO_2-eq of avoided GWP per functional unit, originating from two main sources. First, emissions associated with the disposal of NaOH from waste materials are avoided. Second, the GWP associated with the use of fresh NaOH, as quantified in previous attributional LCA analyses, is mitigated. In particular, the GWP stemming from the disposal processes associated with NaOH waste (at pH 13) can be entirely avoided, with 0.0393 kg CO_2-eq per functional unit being attributed to the disposal of such. In summary, the combined avoided GWP resulting from both the utilization and disposal of NaOH from waste streams totaled 0.1678 kg CO_2-eq per functional unit, representing a 76 % reduction in the total GWP of Scenario 3.

After adsorption, the spent carbon black can be repurposed in the cement industry as a partial substitute for coal in clinker production, promoting circular economy principles [39]. Prior to this application, the 2,4-D-laden CB must undergo high-temperature pyrolysis (>850 °C) with appropriate air pollution control systems to capture HCl and Cl_2 emissions and prevent the formation of toxic byproducts such as dioxins and furans [40]. The repurposed carbon black offers economic advantages with its high heating value of 29,856 kJ/kg—higher than coal (20,327 kJ/kg)—and lower cost (65 USD/ton compared to 84 USD/ton for coal). When blended with coal at 5 % by weight, this approach reduces the global warming potential to approximately 115–117 kg CO_2 eq/ton and decreases clinker production costs by 1–3 % [39].

3.7. Potential operational cost savings

An analysis of the operational costs of the three 2,4-D wastewater treatment scenarios revealed significant cost-saving opportunities associated with substituting fresh chemicals with waste-derived materials. Scenario 1, which involved the use of APTES-modified CB and fresh chemicals for pH adjustment, incurred an operational cost of US $1.49 per functional unit (42 mg of 2,4-D absorbed). In this scenario, the primary cost driver was NaOH, accounting for 89.30 % of the total operational cost, while the APTES represented a minor contribution at 0.0003 %.

Scenario 2, utilizing CB with fresh NaOH, had a slightly lower operational cost of US$1.37 per functional unit, representing an 8.05 % decrease compared to Scenario 1. Similarly to Scenario 1, the primary cost driver in Scenario 2 was the fresh NaOH, which constituted 97.51 % of the total cost.

Conversely, Scenario 3, in which the fresh chemicals were replaced with waste-derived NaOH, showed a dramatic cost reduction. The operational cost for Scenario 3 was estimated at only US$0.09 per functional unit, reflecting a 93.95 % decrease relative to Scenario 2. This substantial saving can be attributed to the substitution of the fresh NaOH with waste-derived NaOH, significantly lowering the overall chemical expense.

This cost comparison underscores the economic viability of utilizing waste materials for pH adjustment in 2,4-D wastewater treatment. By integrating waste-derived NaOH, Scenario 3 not only reduced the dependency on fresh chemicals, but also achieved the lowest operational cost among the three scenarios, marking a transformative step toward more sustainable and cost-effective wastewater treatment practices.

4. Conclusion

A sustainable approach for treating 2,4-D-contaminated wastewater under challenging acidic conditions was presented through the integration of bare CB and waste-derived chemicals in this research. It revealed that the adsorption capacity of bare CB is significantly enhanced at pH 2, compared to neutral conditions. It was revealed in this study that the synergistic effects of hydrogen bonding and electrostatic and Lewis acid–base interactions. At this optimal pH, we identified the ideal CB dosage of 4.5 g/L, beyond which aggregation effects reduced the removal efficiency. The adsorption process followed the Freundlich isotherm and pseudo-second-order kinetic models, indicating multi-layer, heterogeneous adsorption and chemisorption mechanisms.

A comparative sustainability assessment demonstrated that utilizing bare CB at a naturally low pH, coupled with waste-derived NaOH for the final pH adjustment, offered significant advantages over APTES-modified CB at pH 4. While APTES modification achieved a 3.63-times higher sorption capacity, our integrated approach using bare CB with waste-derived NaOH reduced the GWP by 27 % compared to using APTES-modified CB with fresh NaOH. This reduction primarily stemmed from avoiding energy-intensive modification processes and utilizing waste-derived chemicals. Furthermore, the operational costs decreased by 35 % through eliminating modification steps and by substituting fresh chemicals with waste-derived alternatives.

This study provided valuable insights for industries managing acidic wastewaters, demonstrating that leveraging inherent wastewater characteristics (low pH) while incorporating waste-derived materials can enhance both environmental and economic sustainability. This research supported the viability of circular-economy approaches in wastewater treatment, particularly for streams with challenging pH conditions. For industrial applications with complex wastewater compositions, consideration must be given to competing ions and contaminants. While unmodified CB shows limited efficiency for common metal ions and other ionic species, APTES-modified CB can simultaneously remove 2,4-D and various ions through hydrogen bonding and ion exchange mechanisms [41,42]. The efficacy of these adsorption processes is highly pH-dependent, with 2,4-D removal favored at low pH [16] and heavy metal adsorption at higher pH [43]. After adsorption, the spent CB can be repurposed in cement production as a partial coal substitute, undergoing high-temperature pyrolysis (>850 °C) with appropriate emission controls [39,40].Future research should focus on optimizing this method for large-scale application, exploring its efficacy across different complex wastewaters, and developing integrated treatment systems that combine modified CB with complementary processes for comprehensive pollutant elimination.

CRediT authorship contribution statement

Noppaluck Promjan: Writing – original draft, Visualization, Supervision, Project administration, Methodology, Formal analysis, Data curation. **Kullapa Soratana:** Writing – review & editing, Writing – original draft, Visualization, Validation, Supervision, Project administration, Methodology, Investigation, Formal analysis, Data curation, Conceptualization. **Tanapon Phenrat:** Writing – review & editing, Writing – original draft, Visualization, Validation, Supervision, Resources, Project administration, Methodology, Investigation, Formal analysis, Data curation, Conceptualization.

Declaration of competing interest

The authors declare that they have no known competing financial interests or personal relationships that could have appeared to influence the work reported in this paper.

Acknowledgements

This study was supported by a scholarship for the development of middle-aged researchers, Fiscal Year 2020 of the National Research Council of Thailand (NRCT) and Naresuan University (Contact no. วช. อว. (อ) (กบง)/ 290/2563) (Sub-code NRCT6-RSA63011). The authors would like to acknowledge the Thailand Research Fund's financial support through the Royal Golden Jubilee PhD Program (Grant no. PHD/0077/2559).

Appendix A. Supplementary data

Supplementary data to this article can be found online at https://doi.org/10.1016/j.jwpe.2025.108137.

Data availability

Data will be made available on request.

References

[1] F. Islam, J. Wang, M.A. Farooq, M.S. Khan, L. Xu, J. Zhu, W. Zhou, Potential impact of the herbicide 2, 4-dichlorophenoxyacetic acid on human and ecosystems, Environ. Int. 111 (2018) 332–351, https://doi.org/10.1016/j.envint.2017.10.020.
[2] Y. Song, Insight into the mode of action of 2, 4-dichlorophenoxyacetic acid (2, 4-D) as an herbicide, J. Integr. Plant Biol. 56 (2) (2014) 106–113, https://doi.org/10.1111/jipb.12131.
[3] W. Liu, H. Li, F. Tao, S. Li, Z. Tian, H. Xie, Formation and contamination of PCDD/fs, PCBs, PeCBz, HxCBz and polychlorophenols in the production of 2, 4-D products, Chemosphere 92 (3) (2013) 304–308, https://doi.org/10.1016/j.chemosphere.2013.03.031.
[4] N.R. Zuanazzi, N. de Castilhos Ghisi, E.C. Oliveira, Analysis of global trends and gaps for studies about 2, 4-D herbicide toxicity: a scientometric review, Chemosphere 241 (2020) 125016, https://doi.org/10.1016/j.chemosphere.2019.125016.
[5] S. Kwonpongsagoon, C. Katasila, P. Kongtip, S. Woskie, Application intensity and spatial distribution of three major herbicides from agricultural and nonagricultural practices in the central plain of Thailand, Int. J. Environ. Res. Public Health 18 (6) (2021) 3046, https://doi.org/10.3390/ijerph18063046.
[6] C.A. Jote, A review of 2, 4-D environmental fate, persistence and toxicity effects on living organisms, Organic and Medicinal Chemistry International Journal 9 (2019) 22–32, https://doi.org/10.19080/OMCIJ.2019.09.555755.
[7] J. Buenrostro-Zagal, A. Ramirez-Oliva, S. Caffarel-Mendez, B. Schettino-Bermudez, H. Poggi-Varaldo, Treatment of a 2, 4-dichlorophenoxyacetic acid (2, 4-D) contamined wastewater in a membrane bioreactor, Water Sci. Technol. 42 (5–6) (2000) 185–192, https://doi.org/10.2166/wst.2000.0513.
[8] R.G. Zepp, N.L. Wolfe, J.A. Gordon, G.L. Baughman, Dynamics of 2, 4-D esters in surface waters. Hydrolysis, photolysis, and vaporization, Environ. Sci. Technol. 9 (13) (1975) 1144–1150, https://doi.org/10.1021/es60111a001.
[9] H. Canada, Guidelines for Canadian drinking water quality: guideline technical document – 2,4–Dichlorophenoxyacetic acid. From. https://www.canada.ca/en/health-canada/services/publications/healthy-living/guidelines-canadian-drinking-water-quality-guideline-technical-document-2-4-dichlorophenoxyacetic-acid.html, 2023.
[10] E. Bazrafshan, M.F. KORD, H. Faridi, M. Farzadkia, S. Sargazi, A. Sohrabi, Removal of 2, 4-dichlorophenoxyacetic acid (2, 4-D) from aqueous environments using single-walled carbon nanotubes, 2013, https://doi.org/10.17795/jhealthscope-7710.
[11] V.I. Isaeva, M.D. Vedenyapina, S.A. Kulaishin, A.A. Lobova, V.V. Chernyshev, G. I. Kapustin, V.D. Nissenbaum, Adsorption of 2, 4-dichlorophenoxyacetic acid in an aqueous medium on nanoscale MIL-53 (Al) type materials, Dalton Trans. 48 (40) (2019) 15091–15104, https://doi.org/10.1039/C9DT03037A.
[12] R. Jazini Zadeh, M. Sayadi, M.R. Rezaei, Removal of 2, 4-dichlorophenoxyacetic acid from aqueous solutions by modified magnetic nanoparticles with amino functional groups, J. Water Environ. Nanotechnol. 5 (2) (2020) 147–156, https://doi.org/10.22090/jwent.2020.02.005.
[13] T.-H. Lin, Y.-S. Chien, W.-M. Chiu, Rubber tire life cycle assessment and the effect of reducing carbon footprint by replacing carbon black with graphene, Int. J. Green Energy 14 (1) (2017) 97–104, https://doi.org/10.1080/15435075.2016.1253575.
[14] L. Paredes, C. Alfonsin, T. Allegue, F. Omil, M. Carballa, Integrating granular activated carbon in the post-treatment of membrane and settler effluents to improve organic micropollutants removal, Chem. Eng. J. 345 (2018) 79–86, https://doi.org/10.1016/j.cej.2018.03.120.
[15] H.Y. Teah, T. Sato, K. Namiki, M. Asaka, K. Feng, S. Noda, Life cycle greenhouse gas emissions of long and pure carbon nanotubes synthesized via on-substrate and fluidized-bed chemical vapor deposition, ACS Sustain. Chem. Eng. 8 (4) (2020) 1730–1740, https://doi.org/10.1021/acssuschemeng.9b04542.
[16] I. Legocka, K. Kuśmierek, A. Świątkowski, E. Wierzbicka, Adsorption of 2, 4-D and MCPA herbicides on carbon black modified with hydrogen peroxide and aminopropyltriethoxysilane, Materials 15 (23) (2022) 8433, https://doi.org/10.3390/ma15238433.
[17] P.K. Ghosh, L. Philip, Performance evaluation of waste activated carbon on atrazine removal from contaminated water, J. Environ. Sci. Health B 40 (3) (2005) 425–441, https://doi.org/10.1081/PFC-200047576.
[18] N. Liu, A.B. Charrua, C.-H. Weng, X. Yuan, F. Ding, Characterization of biochars derived from agriculture wastes and their adsorptive removal of atrazine from aqueous solution: a comparative study, Bioresour. Technol. 198 (2015) 55–62.
[19] D. Mohan, S. Rajput, V.K. Singh, P.H. Steele, C.U. Pittman Jr., Modeling and evaluation of chromium remediation from water using low cost bio-char, a green adsorbent, J. Hazard. Mater. 188 (1–3) (2011) 319–333.
[20] G. Tan, W. Sun, Y. Xu, H. Wang, N. Xu, Sorption of mercury (II) and atrazine by biochar, modified biochars and biochar based activated carbon in aqueous solution, Bioresour. Technol. 211 (2016) 727–735.
[21] M. Essandoh, D. Wolgemuth, C.U. Pittman Jr., D. Mohan, T. Mlsna, Phenoxy herbicide removal from aqueous solutions using fast pyrolysis switchgrass biochar, Chemosphere 174 (2017) 49–57.
[22] C.C. Novo, L. Senff, M.P. Seabra, R.M. Novais, J.A. Labrincha, The role of an industrial alkaline wastewater in the alkali activation of biomass fly ash, Appl. Sci. 12 (7) (2022) 3612, https://doi.org/10.3390/app12073612.
[23] R. Bradley, I. Sutherland, E. Sheng, Carbon surface: area, porosity, chemistry, and energy, J. Colloid Interface Sci. 179 (2) (1996) 561–569, https://doi.org/10.1006/jcis.1996.0250.
[24] D. Borah, S. Satokawa, S. Kato, T. Kojima, Characterization of chemically modified carbon black for sorption application, Appl. Surf. Sci. 254 (10) (2008) 3049–3056, https://doi.org/10.1016/j.apsusc.2007.10.053.
[25] D. Borah, S. Satokawa, S. Kato, T. Kojima, Surface-modified carbon black for as (V) removal, J. Colloid Interface Sci. 319 (1) (2008) 53–62, https://doi.org/10.1016/j.jcis.2007.11.019.
[26] J. Pena, N. Allen, M. Edge, C. Liauw, B. Valange, F. Santamaría, The use of microwave and FTIR spectroscopy for the characterisation of carbon blacks modified with stabilisers, Polym. Degrad. Stab. 74 (1) (2001) 1–24, https://doi.org/10.1016/S0141-3910(01)00009-X.
[27] A. Anjum, Recovered carbon black from waste tire pyrolysis: characteristics, performance, and valorisation, 2021, https://doi.org/10.3990/1.9789036552899.
[28] J.D. Martínez, N. Cardona-Uribe, R. Murillo, T. García, J.M. López, Carbon black recovery from waste tire pyrolysis by demineralization: production and application in rubber compounding, Waste Manag. 85 (2019) 574–584, https://doi.org/10.1016/j.wasman.2019.01.016.
[29] W. Yang, F. Jiao, L. Zhou, X. Chen, X. Jiang, Molecularly imprinted polymers coated on multi-walled carbon nanotubes through a simple indirect method for the determination of 2, 4-dichlorophenoxyacetic acid in environmental water, Appl. Surf. Sci. 284 (2013) 692–699, https://doi.org/10.1016/j.apsusc.2013.07.157.
[30] J.S. Lazarotto, K. da Boit Martinello, J. Georgin, D.S. Franco, M.S. Netto, D. G. Piccilli, G.L. Dotto, Preparation of activated carbon from the residues of the mushroom (*Agaricus bisporus*) production chain for the adsorption of the 2, 4-dichlorophenoxyacetic herbicide, J. Environ. Chem. Eng. 9 (6) (2021) 106843, https://doi.org/10.1016/j.jece.2021.106843.
[31] S.W. Alberti, K.V. Hübner, C. Busso, E.A. da Silva, F.B. Scheufele, 2, 4-D removal by fish scales-derived carbon/apatite composite adsorbent: adsorption mechanism and modeling, J. Mol. Liq. 382 (2023) 121958, https://doi.org/10.1016/j.molliq.2023.121958.
[32] G. Wu, J. Ma, S. Li, S. Wang, B. Jiang, S. Luo, L. Chen, Cationic metal-organic frameworks as an efficient adsorbent for the removal of 2, 4-dichlorophenoxyacetic acid from aqueous solutions, Environ. Res. 186 (2020) 109542, https://doi.org/10.1016/j.envres.2020.109542.
[33] K. Nuithitikul, S. Srikhun, S. Hirunpraditkoon, Kinetics and equilibrium adsorption of basic green 4 dye on activated carbon derived from durian peel: effects of pyrolysis and post-treatment conditions, J. Taiwan Inst. Chem. Eng. 41 (5) (2010) 591–598, https://doi.org/10.1016/j.jtice.2010.01.007.
[34] X. Chen, G. Chen, L. Chen, Y. Chen, J. Lehmann, M.B. McBride, A.G. Hay, Adsorption of copper and zinc by biochars produced from pyrolysis of hardwood and corn straw in aqueous solution, Bioresour. Technol. 102 (19) (2011) 8877–8884, https://doi.org/10.1016/j.biortech.2011.06.078.
[35] N.S. Trivedi, R.A. Kharkar, S.A. Mandavgane, Utilization of cotton plant ash and char for removal of 2, 4-dichlorophenoxyacetic acid, Resource-efficient technologies 2 (39–46) (2016), https://doi.org/10.1016/j.reffit.2016.11.001.
[36] S. Kalam, S.A. Abu-Khamsin, M.S. Kamal, S. Patil, Surfactant adsorption isotherms: a review, ACS Omega 6 (48) (2021) 32342–32348, https://doi.org/10.1021/acsomega.1c04661.
[37] T.R. Sahoo, B. Prelot, Adsorption processes for the removal of contaminants from wastewater: the perspective role of nanomaterials and nanotechnology *Nanomaterials for the Detection and Removal of Wastewater Pollutants*, Elsevier, 2020, pp. 161–222.
[38] Y. Debebe, E. Alemayehu, Z. Worku, W. Bae, B. Lennartz, Sorption of 2, 4-dichlorophenoxyacetic acid from agricultural leachate using termite mound soil: optimization using response surface methodology, Water 15 (2) (2023) 327, https://doi.org/10.3390/w15020327.
[39] S. Sarawan, T. Wongwuttanasatian, A feasibility study of using carbon black as a substitute to coal in cement industry, Energy Sustain. Dev. 17 (3) (2013) 257–260.
[40] T. Shibamoto, A. Yasuhara, T. Katami, Dioxin formation from waste incineration, Rev. Environ. Contam. Toxicol. (2007) 1–41.
[41] M. Blachnio, K. Kusmierek, A. Swiatkowski, A. Derylo-Marczewska, Adsorption of phenoxyacetic herbicides from water on carbonaceous and non-carbonaceous adsorbents, Molecules 28 (14) (2023) 5404.

[42] J. Wang, H. Liu, S. Yang, J. Zhang, C. Zhang, H. Wu, Physicochemical characteristics and sorption capacities of heavy metal ions of activated carbons derived by activation with different alkyl phosphate triesters, Appl. Surf. Sci. 316 (2014) 443–450.

[43] V. López-Ramón, C. Moreno-Castilla, J. Rivera-Utrilla, L.R. Radovic, Ionic strength effects in aqueous phase adsorption of metal ions on activated carbons, Carbon 41 (10) (2003) 2020–2022.

[44] P. Mooheng, K. Soratana, T. Phenrat, Acid-assisted recycling of iron hydroxide sludge as a coagulant for metalworking fluid wastewater treatment, Waste Biomass Valoriz. 10 (2019) 3635–3645, https://doi.org/10.1007/s12649-019-00696-9.